ARTICLES
https://doi.org/10.1038/s41567-019-0782-3
nature physics

# Classical discrete time crystals

Norman Y. Yao[1,2*], Chetan Nayak[3], Leon Balents[4] and Michael P. Zaletel[1,5]

**The spontaneous breaking of time-translation symmetry in periodically driven quantum systems leads to a new phase of matter: the discrete time crystal (DTC). This phase exhibits collective subharmonic oscillations that depend upon an interplay of non-equilibrium driving, many-body interactions and the breakdown of ergodicity. However, subharmonic responses are also a well-known feature of classical dynamical systems ranging from predator–prey models to Faraday waves and a.c.-driven charge density waves. This raises the question of whether these classical phenomena display the same rigidity characteristic of a quantum DTC. In this work, we explore this question in the context of periodically driven Hamiltonian dynamics coupled to a finite-temperature bath, which provides both friction and, crucially, noise. Focusing on one-dimensional chains, where in equilibrium any transition would be forbidden at finite temperature, we provide evidence that the combination of noise and interactions drives a sharp, first-order dynamical phase transition between a discrete time-translation invariant phase and an activated classical discrete time crystal (CDTC) in which time-translation symmetry is broken out to exponentially long timescales. Power-law correlations are present along a first-order line, which terminates at a critical point. We analyse the transition by mapping it to the locked-to-sliding transition of a d.c.-driven charge density wave. Finally, building upon results from the field of probabilistic cellular automata, we conjecture the existence of classical time crystals with true long-range order, where time-translation symmetry is broken out to infinite times.**

Subharmonic entrainment occurs when the long-time dynamics of a system manifest a period that is a fixed multiple of the period of the underlying equations of motion[1–7]. Such subharmonic behaviour is ubiquitous in deterministic dynamical systems. Most notably, for example, discrete maps, such as $x \to f(x)$, can exhibit stable period-doubled orbits[2,8–10], and continuous-time systems can settle down into limit cycles[7,11]. From the point of view of many-body physics, however, to consider this subharmonic response characteristic of a phase of matter, the system should satisfy certain properties that embody the notion of rigidity. First, the system should have many locally coupled degrees of freedom so that a notion of spatial dimension and thermodynamic limit can be defined. Second, the system's subharmonic response should be stable to arbitrary perturbations of both the initial state and the equations of motion, so long as the latter preserves the periodicity. Models with continuous time-translation invariance, such as the Van der Pol oscillator[11] and the Kuramoto model[12,13], are not rigid in this sense (although the many-body synchronization transition of the latter is of interest in its own right—we comment on its relation to the CDTC problem in the conclusions). Finally, the subharmonic response should have an infinite autocorrelation time, by analogy to 'long-range' order.

Even within the constraints of these criteria, it turns out that general dynamical systems can still exhibit rigid subharmonic entrainment. The reason for this is that the dynamics about fixed points can be strongly damped so that perturbations to either the state or the dynamics decay rapidly. In the presence of such contractive/dissipative dynamics, many-body subharmonic entrainment has been observed in a multitude of systems, including Faraday wave instabilities[3], driven charge density wave materials[4,14–22], and Josephson junction arrays[23,24].

The possibility of rigid subharmonic entrainment in the absence of contractive dynamics is significantly more subtle, but also particularly relevant[25–32]. Indeed, two broad classes of system that fall into this category are time-periodic Hamiltonian dynamics in classical systems and unitary dynamics in quantum systems. Such systems are far more restrictive than general dynamical maps. Hamiltonian dynamics, for example, are volume preserving in phase space, thereby explicitly forbidding contractive dynamics. In the presence of an external drive (for example, which sets the periodicity of the dynamics), energy conservation is broken and one generically expects the long-time dynamics of the many-body system to be completely ergodic. In certain fine-tuned special cases[33,34], it may be possible for a driven, many-body system to avoid its ergodic fate[35]. An ergodic system can never exhibit true subharmonic rigidity because it is impossible for the system to remember in which of the distinct subharmonic orbits (related by time-translation symmetry) it began.

To this end, a tremendous amount of recent excitement has focused on the discovery that rigid subharmonic entrainment can occur in a periodically driven (Floquet), unitary, many-body quantum system. Dubbed discrete time crystals[36–44], this new phase of quantum matter relies crucially on many-body localization (MBL) to prevent the drive-induced heating of the system to infinite temperature. Although it is difficult to experimentally verify the long-time rigidity associated with a discrete time crystal, promising signatures of such behaviour have been observed in spin systems[45,46] for timescales up to hundreds of Floquet cycles, despite the fact that localization is probably absent in such systems[43,46–48].

A natural question thus arises: how quantum must a time crystal truly be? Is quantum mechanics important only insofar as it allows for MBL to prevent heating of the system? Or does it play a more fundamental role? If closed Hamiltonian dynamics cannot generically stabilize a time crystal due to heating, a natural generalization is to consider preventing such heating by coupling the system to a bath, most simply by adding friction. However, by adding only friction, one essentially reverts back to the damped case where the existence of rigid subharmonic entrainment is well known.

[1]Department of Physics, University of California Berkeley, Berkeley, CA, USA. [2]Materials Science Division, Lawrence Berkeley National Laboratory, Berkeley, CA, USA. [3]Station Q, Microsoft Research, Santa Barbara, CA, USA. [4]Kavli Institute of Theoretical Physics, University of California, Santa Barbara, CA, USA. [5]Department of Physics, Princeton University, Princeton, NJ, USA. *e-mail: norman.yao@berkeley.edu

On the other hand, if the bath is in equilibrium at finite temperature $T$, the fluctuation-dissipation theorem implies that friction must come with noise[49]. In classical systems, this noise can be captured as a Langevin force, $F_B(t) = -\eta\dot{q} + \xi(t)$, on each coordinate $q$, where $\eta$ is the strength of the friction and $\xi(t)$ is a stochastic force with variance, $\langle \xi(t)\xi(t')\rangle = 2\eta T\delta(t-t')$. Taking $\eta > 0$, $T = 0$ reduces to the damped case where period-doubling is easily stabilized, while a combination of finite $T$ and driving results in a truly non-equilibrium situation. The question concerning the existence of 'classical discrete time crystals' (CDTC) can then be posed as follows: in what dimensions can a classical many-body system, coupled to an equilibrium bath, exhibit rigid subharmonic entrainment for either the closed case ($\eta = 0$), the zero-temperature case ($\eta > 0$, $T = 0$) or the finite temperature case ($\eta$, $T > 0$)?

Because the $T = 0$ (no noise) case is already known to feature rigid subharmonic entrainment, in this work we focus on $T > 0$. Furthermore, if a CDTC exists in $d_*$ dimensions, it will presumably exist for all $d \geq d_*$, so we focus on the most delicate case: $T > 0$ in one dimension (1D). Although an equilibrium phase transition is impossible in 1D, might there nevertheless be a non-equilibrium dynamical phase transition between a period-doubled CDTC and a symmetric phase?

In this work, we first argue, based on remarkable results due to Gács[50–52] and Toom[53–55], that in principle true CDTCs, with an infinite autocorrelation time, are possible in all dimensions $d > 0$ (ref. [56]). However, in 1D the construction is so baroque that we cannot yet explicitly prove this conjecture theoretically or numerically. To this end, we instead investigate in detail a more physical Hamiltonian, the parametrically driven Frenkel–Kontorova (FK) model. The basic idea is simple: each nonlinear oscillator in the chain undergoes a 2:1 parametric resonance, and we couple the oscillators together to try and stabilize the CDTC phase at finite temperature. We find that this model exhibits an intriguing line of first-order dynamical phase transitions, between an 'activated' period-doubled CDTC and a symmetry-unbroken phase, that terminates at a critical point (Figs. 1 and 2). The activated CDTC is not a true time crystal; rather, it has has an autocorrelation time that diverges exponentially as $T \to 0$. Because of this exponentially diverging timescale, it would be extremely difficult in experiments to distinguish between an activated CDTC and a true, long-range-ordered CDTC; indeed, to detect this difference we must conduct careful numerical experiments over many millions of Floquet cycles.

Before diving into the details, let us emphasize the key characteristic of a true long-range-ordered CDTC, namely, the existence of period-doubling with an infinitely long autocorrelation time $\tau$, which is stable to small perturbations of the dynamics. More precisely, if one considers a model of periodically driven oscillators with position coordinates $q_i$, the autocorrelation time $\tau$ of period-doubling can be quantified as $\langle q_i(nt_D)q_i(0)\rangle \propto (-1)^n e^{-nt_D/\tau}$, where $t_D$ is the period of the drive and $\langle\ \rangle$ indicates averaging over noise realizations. For low but finite temperatures, the period-doubling we observe in the driven FK model exhibits only an activated autocorrelation time, $\tau(T) \approx e^{\Delta_{eff}/T}$, where $\Delta_{eff}$ is an effective activation barrier. Thus, in 1D, the CDTC order of the FK model we study survives only to exponentially long, but not infinite times. Despite the activated behaviour of the period-doubling, we nevertheless find a first-order dynamical phase transition where $\tau(T)$ drops discontinuously and period-doubling is completely destroyed (Fig. 2). In 1D, such a first-order phase transition would be impossible in equilibrium[57].

This leaves the question of CDTCs at a peculiar point: although we believe a true CDTC is in principle possible in 1D, the obvious candidate model is only exponentially close to one. It may be that the full complexity of Gács' construction, which we now explain, is in fact required.

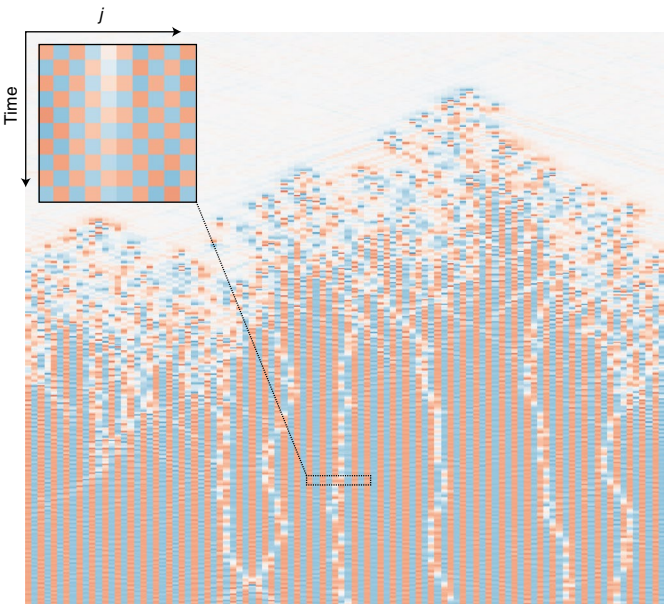


**Fig. 1 | Period-doubled dynamics 'boil' out of a uniform initial state.** In the main panel we present a stroboscopic view $q_j(2nt_D)$, with time $n$ running down vertically ($0 < n < 1{,}200$) and space $j$ running horizontally over the $n_{osc} = 100$ oscillators. The colour scale shows $q_j < 0$ as red, $q_j > 0$ as blue and $q_j \approx 0$ as white. Note that we strobe every two driving periods, which is the frequency of the subharmonic response. Hence, the displayed phase of the oscillators varies slowly. A detail of a smaller region strobed at the driving frequency, $q_j(nt_D)$, is shown in the inset. The period-doubled oscillations $q_j(nt_D) \propto (-1)^n$ are now manifest. Strikingly, the correlations are antiferromagnetic both in time and space, even though the oscillators are coupled together ferromagnetically ($\omega_D = 1.958$, $g = 0.065$, $\delta = 0.067$, $\eta = 0.003$, $T = 0.004$). In the final state, there is a finite density of $\pi$-domain walls between the two different period-doubled solutions.

**Conjecture on the existence of classical time crystals.** Although our ultimate interest is to understand the possibility of time crystals in open Hamiltonian systems, it is first worth considering a more general class of dynamical systems, 'probabilistic cellular automata' (PCA). Recall that a deterministic cellular automata (CA) is a set of spins $\{\sigma_i\}$, where $\sigma_i \in \{1, 2, ..., N\}$, with a discrete update rule $\sigma_i \to T[\sigma_{i-1}, \sigma_i, \sigma_{i+1}]$[58]. In a PCA, the system is instead described by a probability distribution $\mathcal{P}[\{\sigma_i\}]$ over spin configurations, which is updated by a local Markov process; that is, each $\sigma_i$ is updated with a probability distribution that depends only on itself and its neighbours. One way to obtain a PCA is to start with a deterministic CA and perturb it by stochastic errors; for example, with probability $E \ll 1$, a spin can violate the transition rule and flip into a random state (the precise statement of such an error model can be found in ref. [51]).

Given that the PCA update rule is discrete time-translation-invariant, one can then ask if the long-time probability distribution can ever oscillate with period two, thereby realizing a time crystal. For a deterministic CA, a time crystal is trivially obtained by letting binary spins transform under the rule $0 \leftrightarrow 1$ (this is analogous to our previous discussion of fine-tuning, or introducing friction but no noise). However, any infinitesimal rate of errors will desynchronize the spins and the autocorrelations will decay over a timescale $\tau \sim 1/E$.

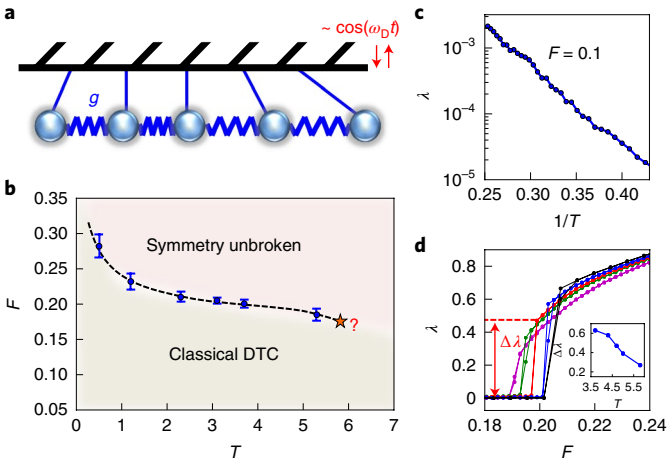


**Fig. 2 | Diagnostics and phase diagram of an activated classical discrete time crystal. a**, Schematic of a one-dimensional (1D) array of coupled nonlinear pendula. The pendula are coupled via ferromagnetic interactions of strength $g$, and the system is parametrically driven at frequency $\omega_D$. **b**, Phase diagram of the classical discrete time crystal as a function of $F=\frac{2\eta}{\delta}$ (where $\delta$ is the driving amplitude and $\eta$ the damping) and temperature $T$. At low $T$ there is a first-order phase transition between the CDTC phase and the non-time-crystalline phase, while at high $T$ there is only a crossover. **c**, In the 1D CDTC, there is a finite rate of phase slips $v$ between the two symmetry-breaking solutions. $v$ fits very well to the Arhennius form $v\approx e^{-\Delta/T}$, indicating the phase slips are activated. **d**, The phase transition is diagnosed by measuring the rate of phase slips $v$ between the two time-translation-related period-doubled solutions. As we cross the first-order line out of the CDTC, $v$ jumps discontinuously.

Might there be a more complicated CA that implements 'error correction', enabling the system to preserve long-range (time-crystalline) order? The most obvious guess is to have each spin poll its neighbours and transition opposite to the majority, essentially implementing a type of ferromagnetism. This 'anti-majority vote' rule, it turns out, is insufficient to preserve the long-range order, because if a pair of domain walls nucleates and separates beyond the range of the vote, they will diffuse randomly throughout the system and destroy the order.

For a very long time it was thought that such error correction was in fact impossible in 1D as a consequence of the so-called 'positive rates conjecture'. A PCA is said to be 'ergodic' if it has a unique fixed-point probability distribution $\mathcal{P}_0[\{\sigma_i\}]$. The positive rates conjecture states that a PCA is generically ergodic, generalizing the physics folklore regarding the impossibility of ferromagnetism in 1D to the non-equilibrium setting[35]. On the other hand, the infinite autocorrelation time of a time crystal requires ergodicity breaking, because there will be two probability distributions $\mathcal{P}_\pm[\{\sigma_i\}]$, corresponding to the two phases ($\sigma_i=\pm1$) of the period-doubling, invariant under a double Markov update. Consequently, were the positive rates conjecture true, it would forbid time crystals as a corollary.

However, almost two decades ago, a truly remarkable counter-example to the positive rates conjecture was provided by Gács[50–52]. Gács constructed a 1D PCA with the following property: in the thermodynamic limit, there is a threshold error-rate $E<E_*$, below which a system of size $L$ has $2^L$ distinct steady states in the thermodynamic limit; that is, it 'remembers' one bit per unit cell. Admittedly, the Gács PCA is very complicated: each cell has a state space whose dimension is on the order of $\sigma_i\in\{1, 2, ..., 2^{400}\}$, which one can think of as 399 ancillary bits that implement an error correction protocol on one protected bit. The error correction is a highly collective phenomenon, requiring communication (interactions) between neighbouring cells because there are occasional error events that scramble all constituent 400 bits simultaneously. The error correction is stable against generic perturbations (for example, the errors can be adversarially biased towards a particular spin configuration, breaking anything like an Ising symmetry), so is truly a feature of a new non-equilibrium phase. This is somewhat analogous to MBL, insofar as the ergodicity breaking is extensive and stable to arbitrary perturbations, but is even stronger because the system is open (noisy). Furthermore, the Gács PCA can be used to simulate any deterministic CA acting on the protected subspace. Thus, by using the Gács PCA to simulate the trivial $0\leftrightarrow1$ CA, one obtains an example of a true classical time crystal that is stable against arbitrary stochastic perturbations.

We conjecture that Gács' results with PCAs implies the existence of true CDTCs in time-periodic Hamiltonian Langevin dynamics, because the latter can be used to approximately simulate a discrete PCA. By 'simulate', we mean that if we interpret the integer part of a classical oscillator $q_i$ as the state of a discrete CA, $\sigma_i=q_i$, then by an appropriate choice of time-dependent Hamiltonian and Langevin friction, the dynamics of $q_i$ under one Floquet cycle can mimic the discrete update of a CA. Langevin noise then introduces stochastic errors analogous to those of the PCA. Simulating Gács' PCA in this way would then realize a time crystal as discussed above, and small errors in the 'simulation' would be covered by Gács' stability result.

However, at present this remains a conjecture, rather than a proof, because a priori it is unclear whether the errors arising from Langevin noise can be successfully mapped onto the error model covered in Gács' result. Although we would like to numerically verify this possibility, the Gács model is so complex it is daunting to implement even as a PCA, let alone simulate via continuous-time Langevin dynamics. However, given that we conjecture a CDTC is in principle possible, it is tempting to assume that by writing down a sufficiently general model, we will find this behaviour somewhere in its phase diagram.

**Period-doubling in the FK model.** For concreteness, let us consider a parametrically driven FK model, which describes an array of coupled, nonlinear pendula (Fig. 2a)[59,60]:

$$H=\sum_i \frac{1}{2}p_i^2+[1+\delta\cos(\omega_D t)](1-\cos(q_i))+g\sum_{\langle i,j\rangle}\frac{(q_i-q_j)^2}{2} \quad (1)$$

where $q_i$ is the pendulum's deflection from vertical and $p_i$ its momentum, while $\delta$ and $\omega_D$ are the amplitude and frequency of the parametric driving (Fig. 2a). Such a model can be realized in many different experimental systems (see Supplementary Information). Note that we have normalized each pendulum's natural frequency to one. When $\omega_D\approx2$ and $g=0$ (decoupled), each pendulum is susceptible to a 2:1 parametric resonance, where the dynamics are period-doubled and the pendulum's position returns only once every two driving cycles. Although this subharmonic response (at $\omega_D/2$) is reminiscent of the behaviour expected for a CDTC, the parametric resonance of a single oscillator does not exhibit the rigidity of a true time crystal; rather, as we shall see, this subharmonic response of a single oscillator is destroyed in a smooth crossover for any amount of noise ($T>0$). However, crucially, in the presence of interactions ($|g|>0$), the subharmonic response of the collective system can undergo a sharp transition at $T>0$ characteristic of a many-body phase.

We introduce friction $\eta$ and finite temperature $T$ through a Langevin force $F_B(t)$, which acts independently on each $q_i$. The pendula then evolve under a combination of this stochastic Langevin force and the ferromagnetic ($g>0$) Frenkel–Kontorova Hamiltonian:

$$\frac{dq_i}{dt}=p_i \quad (2)$$

$$\frac{\mathrm{d}p_i}{\mathrm{d}t} = -(1+\delta\cos(\omega_D t))\sin(q_i) + g(q_{i+1}+q_{i-1}-2q_i) - \eta p_i + \xi_i(t) \quad (3)$$

where $\xi_i(t)$ is a stochastic force with variance $\langle \xi_i(t)\xi_j(0)\rangle = \delta_{ij}\delta(t)2\eta T$.

To probe the resulting dynamics, at time $t=0$ we initialize the oscillators in $p_i(0)=q_i(0)=0$ and integrate the equations of motion using a second-order Langevin time-stepper (see Supplementary Information). The resulting stroboscopic dynamics, $q_i(mt_D)$ (where $t_D=2\pi/\omega_D$), are depicted in Fig. 1. Strikingly, the uniform initial condition gives way to a growing bubble of spatio-temporal 'antiferromagnet' in which $q_i(mt_D)\propto(-1)^{i+m}$; these spatial antiferromagnetic correlations are particularly surprising, given that the oscillators are ferromagnetically coupled. The existence of a growing bubble would seem to suggest the presence of two distinct dynamical regimes—time-crystalline and not—despite the finite temperature fluctuations.

**Analysis of a single nonlinear pendulum.** To begin, let us review the parametric resonance of a single nonlinear pendulum[7]. Readers familiar with the resulting phase diagram (Fig. 3) can skip to our discussion of their coupled behaviour, although the treatment in action-angle variables is not entirely standard and will prove illuminating[61]. In the action-angle coordinates of the pendulum, $q\sim\sqrt{2J}\cos(\theta)$, $p\sim-\sqrt{2J}\sin(\theta)$, the Hamiltonian (equation (1)) reduces to

$$H(t) = J - \frac{\epsilon}{2}J^2 + \delta J\cos(\omega_D t)\cos^2(\theta) + \cdots \quad (4)$$

where $\epsilon=\frac{1}{8}$ and higher-order terms in $J$, $\delta$ are neglected[62]. In the undriven case, $\omega(J)=\partial_J H$ sets the frequency of oscillations, so that the nonlinearity is encoded in the $J^2$ term. Because $\epsilon>0$, larger amplitude oscillations have lower frequency; however, we can be more general by keeping $\epsilon$ as a parameter and indeed will later explore the $\epsilon<0$ regime.

Near a period-doubled solution, $q_i \propto \cos(\omega_D t/2+\tilde{\theta})$, where $\tilde{\theta}$ varies slowly. To this end, we transform to the rotating frame, $\tilde{\theta}=\theta-\omega_D t/2$, wherein equation (4) becomes

$$H(t) = (1-\omega_D/2)J - \frac{\epsilon}{2}J^2 + \frac{\delta}{4}J\cos(2\tilde{\theta}) + \frac{\delta}{4}J\left[\cos(2\omega_D t+2\tilde{\theta})+2\cos(\omega_D t)\right] \quad (5)$$

At leading order in a Floquet–Magnus expansion, the average Hamiltonian over a driving period is given by

$$\overline{H} = \frac{1}{t_D}\int_0^{t_D} H(t)\mathrm{d}t \quad (6)$$

$$= \delta(1+u)J/4 - \frac{\epsilon}{2}J^2 + \frac{\delta}{4}J\left(\cos(2\tilde{\theta})-1\right) \quad (7)$$

where $u=4(1-\omega_D/2)/\delta$ is an effective detuning. The static $\overline{H}$ will govern the slow dynamics $\tilde{\theta}$. Although this treatment is approximate (that is, we neglect the off-resonant oscillatory terms), for a single pendulum one can in principle apply a convergent sequence of canonical transformations to bring the Hamiltonian to such a static form, a consequence of the Kolmogorov–Arnold–Moser theorem for small $\delta$ (ref. [61]). The equal-energy contours of $\overline{H}$ are illustrated in Fig. 3a. For $\epsilon>0$, the landscape is that of an inverted double well potential with maxima at $\bar{J}=\epsilon^{-1}(1+u)\frac{\delta}{4}$ and $\tilde{\theta}=0,\pi$, which are the two possible phase shifts of the period-doubled solutions: $q(mt_D)=\pm\sqrt{2\bar{J}}\,(-1)^m$. Because these solutions occur at maxima, perturbations about the orbit remain bounded, oscillating at an effective frequency $\omega_{\mathrm{eff}}^2=\delta^2(1+u)/4$. For weak driving $\delta$, $\omega_{\mathrm{eff}}/\omega_D$ is parametrically small, implying that higher-order terms in our Floquet–Magnus expansion are strongly off-resonant, justifying our approach. We note that period-doubled solutions exist only when $\bar{J}>0$, yielding the period-doubling criterion $u>-1$. Finally, for $\epsilon<0$, the above analysis remains essentially identical except that the period-doubled solutions occur at the minima of $\overline{H}$.

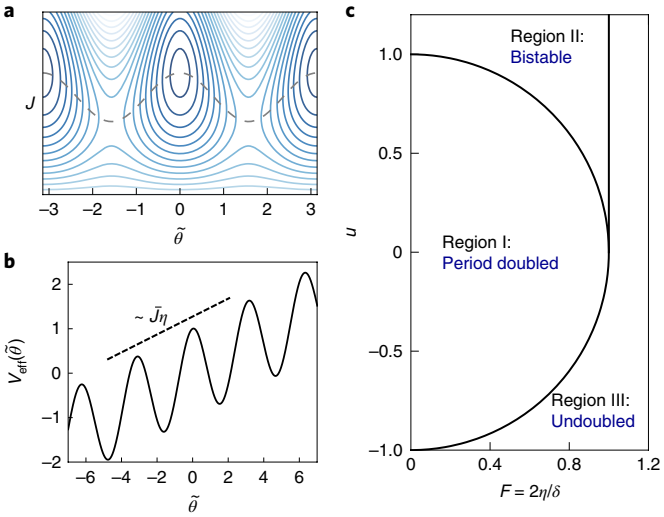


**Fig. 3 | Parametric resonance of a single nonlinear pendulum. a**, Equal pseudoenergy contours of the averaged Hamiltonian $\overline{H}$ in the $\tilde{\theta}, J$ plane. The dashed line indicates the contour $\partial_{\tilde{\theta}}\overline{H}=0$. **b**, Effective washboard potential of equation (10). The slope of the potential arises from the Langevin damping $\eta$. **c**, In region I ($F>1$ or $u<\sqrt{1-F^2}$), the particle slides and there is no period-doubling. In region III, $F<1$, $u>1-F^2$, only the locked (period-doubled) phase is stable. In region II, $F<1$, $u^2<1-F^2$, both the locked and sliding states are stable, implying bistability.

The double well potential has a phase-shift symmetry, $\tilde{\theta}\to\tilde{\theta}+\pi$, which is unrelated to the $q\to-q$ symmetry of the original Hamiltonian, and is actually a more general consequence of period-doubling: in the rotating frame, $\tilde{\theta}\to\tilde{\theta}+\pi$ must remain a dynamical symmetry because it corresponds to time-translation symmetry, $t\to t+t_D$. In fact, the $q\to-q$ symmetry of the original Hamiltonian is inessential to the period-doubling physics we discuss, analogous to the quantum case[38].

To understand the effect of the bath, consider the equations of motion when averaging the Langevin force over one period (see Supplementary Information):

$$\dot{\tilde{\theta}} = \partial_J\overline{H} \quad (8)$$

$$\dot{J} = -\partial_{\tilde{\theta}}\overline{H} - \eta J + \sqrt{\bar{J}}\,\xi(t) \quad (9)$$

In the limit of large detuning relative to the driving ($u\gg1$), these equations take a particularly simple form (see Supplementary Information for the general case):

$$\overline{H} = -\frac{\epsilon\tilde{J}^2}{2} + \bar{J}\left[\frac{\delta}{4}\cos(2\tilde{\theta}) + \eta\tilde{\theta}\right] + \cdots \quad (10)$$

$$\dot{\tilde{\theta}} = \partial_{\tilde{J}}\overline{H} \quad (11)$$

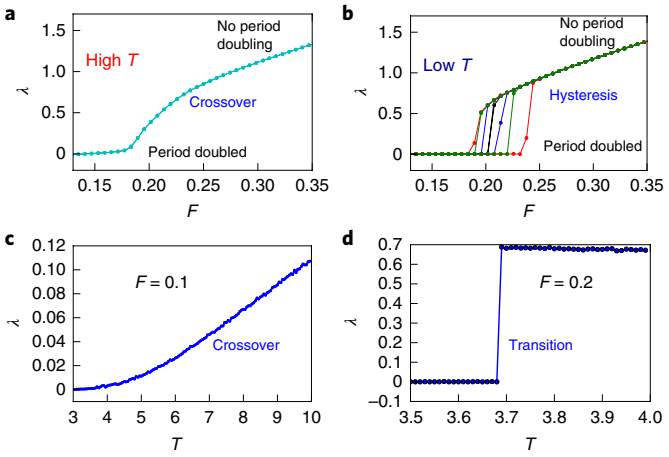


**Fig. 4 | Characterizing the CDTC phase transition by measuring the rate of phase slips, $v = \langle \dot{\tilde{\theta}} \rangle$, as a function of damping $F$ and temperature $T$.** **a**, Characterization for high temperature ($T = 7$). For low damping $F$, $v \approx 0$, indicating period-doubling, while at large $F$, $v > 0$, indicating that a finite rate of π-phase slips destroys true long-range order in time. There is a smooth crossover between these two regimes, with no evidence of hysteresis. **b**, At lower temperatures ($T = 3.7$), we observe a hysteresis loop that closes into a jump discontinuity as we increase the simulation time. Curves of different colour correspond to simulations of length $n_{\text{step}} \in (5\times10^3, 3\times10^4, 3\times10^5, 3\times10^6)$ for each value of $F$ as we sweep up and down. This suggests a first-order non-equilibrium phase transition. **c**,**d**, Analogously, we can hold $F$ fixed and vary $T$. At $F = 0.1$ (**c**), $v$ displays a crossover, while at $F = 0.2$ (**d**), there is a sharp transition. Repeating this analysis throughout the ($F$, $T$)-plane allows us to trace out a first-order line that terminates, yielding the phase diagram in Fig. 2b.

$$\dot{\tilde{J}} = -\partial_{\tilde{\theta}} \overline{H} - \eta \tilde{J} + \sqrt{\overline{J}}\,\xi(t) \tag{12}$$

where $\tilde{J} = J - \overline{J}$ and $\overline{J} = \epsilon^{-1} u \frac{\delta}{4}(1 + \mathcal{O}(u^{-1}))$. These equations describe a negative mass particle with 'position' $\tilde{\theta}$ and 'momentum' $\tilde{J}$ subject to Langevin damping and a washboard potential with finite slope $\overline{J}\eta$, as shown in Fig. 3b. We note that such equations of motion are extremely well studied in the context of *RC*-shunted driven Josephson junctions[63,64], where they can give rise to fractional Shapiro steps[23,24], but our interest will be in their many-body behaviour in the presence of noise[21].

At zero damping, the barrier height of the washboard potential is $\overline{J}\delta/2$, but as the damping $\overline{J}\eta$ increases the barrier height decreases. Thus, to parameterize the damping we consider a dimensionless 'force', $F = \frac{2\eta}{\delta}$, defined so that when $F \geq 1$ the stable extrema vanish and the particle slides along the washboard. In the fully sliding state, $\dot{\tilde{\theta}} = \frac{\delta}{4} u$, which in the original variables gives $\dot{\theta} = 1$, the natural frequency of the undriven oscillator (see Supplementary Information). Thus, the 'sliding regime' indicates the destruction of period-doubling, while the 'locked' regime ($\dot{\tilde{\theta}} = 0$) is period-doubled.

This point is worth emphasizing. Naively, given that the undamped equation (7) is the sine-Gordon representation of the Ising model, it might seem that period-doubling is analogous to the breaking of the internal Ising symmetry generated by $\tilde{\theta} \to \tilde{\theta} \pm \pi$, so that the destruction of the CDTC would occur through something like an Ising transition. However, unlike an Ising model, the friction-induced slope gives π-phase slips a handedness (that is, they in fact have a $\mathbb{Z}$ character rather than a $\mathbb{Z}_2$ Ising character): $\tilde{\theta} \to \tilde{\theta} + \pi$ is inequivalent to $\tilde{\theta} \to \tilde{\theta} - \pi$, and the phase prefers to slip one way. The actual dynamical CDTC phase transition we will observe is a collective version of the locked-to-sliding transition at which $\frac{d\tilde{\theta}}{dt}$ jumps, not an Ising transition, and hence is fundamentally distinct from the transition discussed in the context of the quantum MBL/prethermal time crystal[39,65]. In the Supplementary Information, we demonstrate that this effect is real for the original driven pendulum.

In the absence of noise ($T = 0$), a standard stability analysis[7] reveals three distinct dynamical regimes (Fig. 3c). In region I, only the sliding regime is stable, indicating that there is no period-doubling. In region III, only the locked regime is stable, indicating period-doubling. Finally, region II is a bistable regime in which both the locked and sliding states are stable, and the long-time behaviour depends on the initial state. This region will show hysteresis as $F$ is varied.

At any finite temperature $T > 0$, activated processes cause a single pendulum to transition between the locked and sliding states, by analogy to Kramer's analysis of noise-activated tunnelling[66–68]. This destroys the bistable region II, leading to a smooth (though highly nonlinear) crossover between the locked and sliding regimes as either the force ($F$) or temperature ($T$) is increased[67]. This crossover in the effective static model is consistent with our numerical experiments on the original parametrically driven pendulum (equation (3) and Supplementary Information). Thus, for $g = 0$ (that is, in 0D) and at finite $T$ there is no sharp transition between period-doubled and undoubled dynamics.

**Collective behaviour of coupled nonlinear pendula.** With the single pendulum analysis behind us, let us now turn to the collective behaviour of the system at finite coupling strength $g$.

As before, to analyse the interactions within an effective static model we average the couplings over one Floquet period, $\overline{H}_g = -g \sum_i \sqrt{J_i J_{i+1}} \cos(\tilde{\theta}_i - \tilde{\theta}_{i+1})$ (see Supplementary Information), leading to the effective equations of motion:

$$\overline{H} = \sum_i \left( -\frac{\epsilon \tilde{J}_i^2}{2} + \overline{J}\left[\frac{\delta}{4}\cos(2\tilde{\theta}_i) + \eta\tilde{\theta}_i\right] - g\overline{J}\cos(\tilde{\theta}_i - \tilde{\theta}_{i+1}) \right) \tag{13}$$

$$\dot{\tilde{\theta}}_i = \partial_{\tilde{J}_i} \overline{H} \tag{14}$$

$$\dot{\tilde{J}}_i = -\partial_{\tilde{\theta}_i} \overline{H} - \eta \tilde{J}_i + \sqrt{\overline{J}}\,\xi_i(t) \tag{15}$$

where we have taken $J_i \approx \overline{J} + \mathcal{O}(1/u)$. Except for the negative mass and the finite slope $\eta\tilde{\theta}_i$, these equations correspond to the sine-Gordon representation of the Ising model at finite $T$.

Before exploring the CDTC phase transition in this model, a few remarks are in order. First, at finite damping and zero temperature ($\eta > 0$, $T = 0$), the 1D chain will rather trivially exhibit many-body period-doubling, which is inherited from the period-doubling (region I) of the single oscillator case. Roughly speaking, if we perturb about the period-doubled solution of a single oscillator $q(t)$, $q_j(t) = q(t) + \Delta q_j(t)$, in the limit $g$, $\delta \to 0$ the linearized dispersion relation of the perturbation is strongly off-resonant with the drive, $\omega_{\text{eff}}(k)/\omega_{\text{D}} \sim \delta$, so the finite damping $\eta$ prevents heating and the system settles into a period-doubled steady state, as can be analysed from the stability of the linearized equations of motion.

Second, the negative mass explains why the ferromagnetically coupled pendula exhibit antiferromagnetic spatial synchronization in Fig. 1. Because the period-doubled orbit of a single pendulum occurs at a maximum of $\overline{H}$, the volume of available phase space increases as the quasi-energy decreases. Interpreting this as a relation between entropy and energy, the period-doubled solution is at

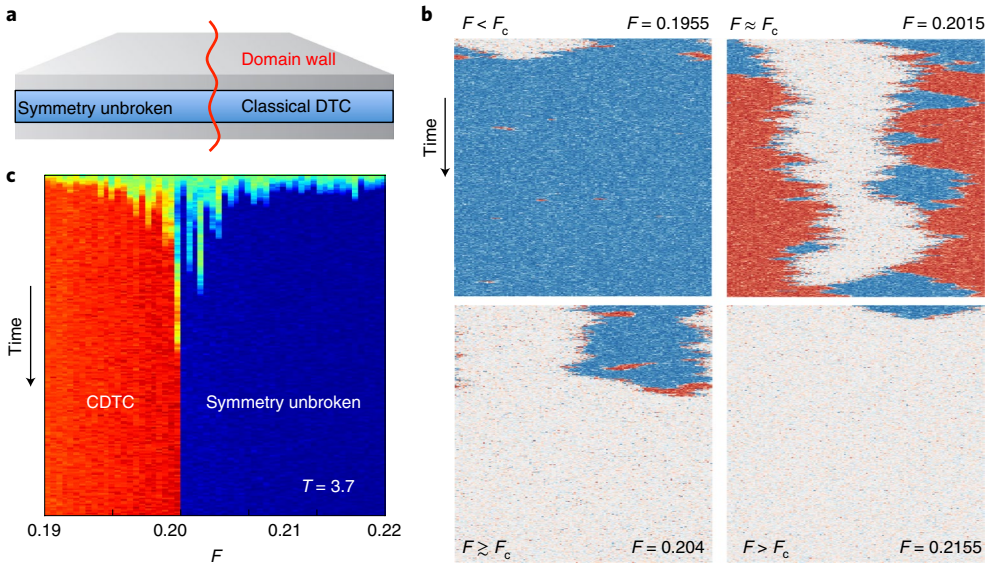


**Fig. 5 | Competition between period-doubled and undoubled dynamics near the putative first-order transition. a**, By introducing a DDW between the two regimes by hand, we circumvent the exponentially large timescale that leads to hysteresis. **b**, Similar to Fig. 1, we present $q_j(2nt_D)$ for $n_{osc}=10^3$ oscillators. We strobe every two driving periods to avoid plotting the period-doubled oscillations. Thus the red and blue regions indicate one or the other period-doubled orbits, while in white regions there is no period-doubling. At $t=0$, we initialize a DDW using an initial state in which $q_j(0)=0$ (left half) or $q_j(0)\approx\sqrt{2J}$ (right half), and then evolve for $n_{steps}=10^6$ periods. If a first-order transition exists at critical force $F_c$, we expect a sensitive dependence of the DDW dynamics on $F$ near the transition. Indeed, for $F<F_c$, the period-doubled region expands and 'eats' the non-time-crystalline region, while for $F>F_c$ we see the opposite. Meanwhile, close to the transition point ($F_c\approx0.2015$ for this particular $T$), the competition between the two phases extends for many steps. **c**, To locate the transition precisely, we use a colour plot to display the time evolution of the average oscillation amplitude $\langle J(t)\rangle_F$ during the DDW quench. Because $\langle J\rangle$ differs in the two regimes, the long-time behaviour converges to one of two possible values as one or the other domain 'wins'.

negative temperature, even though the Langevin bath is at positive temperature. Thus, the array is entropically driven toward a high quasi-energy state, reversing the expected effect of the coupling $g$. To test this hypothesis, we can change the effective mass to be positive by changing the nonlinearity $\epsilon$ of the pendulum (for example, by replacing $\cos(q)\to\frac{1}{2}q^2+\frac{1}{24}q^4$, giving $\epsilon=-\frac{1}{8}$). The period-doubled solutions now exist at minima of $\overline{H}$, corresponding to positive temperature, and analogous simulations indeed show that the pendula now synchronize ferromagnetically (see Supplementary Information). Although negative temperatures are familiar in models with finite phase space[69–71], the parametric resonance of a nonlinear pendulum provides a novel way to dynamically generate negative temperatures in a system with an unbounded phase space. This phenomenon is distinct from the dynamically stabilized inverted position of a Kapitza pendulum, which remains at a minimum of the quasi-energy; indeed, ferromagnetically coupled Kapitza pendula will synchronize ferromagnetically[72].

**CDTC phase transition.** Although $\epsilon>0$ provides access to an intriguing negative temperature regime, from the perspective of time-translation symmetry breaking, the sign of $\epsilon$ does not appear to impact the CDTC. Thus, for the sake of simplicity and to simplify the visual presentation, we will replace the oscillator potential $\cos(q)\to\frac{1}{2}q^2+\frac{1}{24}q^4$ (leading to $\epsilon=-\frac{1}{8}$ and hence ferromagnetic spatial synchronization) for the remainder of the text.

In the absence of a slope, $\eta\tilde{\theta}_i$, in the washboard potential, the effective model is the sine-Gordon representation of the equilibrium 1D Ising model, implying that at finite temperature there will always be a finite density $\sim e^{-g_{eff}/T}$ of $\pi$-domain walls in space, as well as a finite rate of $\pi$-phase slips $\sim e^{-\Delta_{eff}/T}$ in time, where $g_{eff}$ and $\Delta_{eff}$ are effective quasi-energy barriers. This is the reason why in 1D one naively expects that the CDTC phase will exhibit an 'activated' autocorrelation time, $\tau\approx e^{\Delta_{eff}/T}$, with only a smooth crossover in $T$ as in 0D. However, because of the finite slope $\eta\tilde{\theta}_i$ in the washboard potential, this equilibrium intuition need not apply. Indeed, there is evidence that the 1D d.c.-driven FK model (d.c.-driving meaning a finite slope $\eta\tilde{\theta}_i$) shows a first order locked-to-sliding transition at finite temperature[60,73–75], which would map onto a non-equilibrium phase transition between an activated CDTC and a symmetry-unbroken state.

To investigate this possibility numerically, we explore the system's behaviour as a function of both temperature $T$ and the dimensionless 'force' $F$, associated with the washboard slope. To reduce the number of parameters we fix $\eta=0.005$, set $\delta=2\eta/F$, and for each $F$ we adjust $\omega_D$ and $g$ to keep fixed $\omega_{eff}=0.1$ and $g=1.25\delta$. This choice ensures that, throughout the phase diagram, we explore $u\gg1$, $F<1$, so that the oscillators are individually in the bistable regime (region II).

A quantitative diagnostic of period-doubling is given by the 'velocity' parameter, $v=\langle\dot{\tilde{\theta}}\rangle$, where the average is taken over time, space and different realizations of the stochastic force. Period-doubling corresponds to the locked state where $v=0$, while $v\neq0$ (sliding state) implies a finite rate of phase slips and (strictly speaking) the destruction of true period-doubling.

Several representative cuts of $v(F, T)$ in the $(F, T)$-plane are depicted in Fig. 4, and exhibit two regimes. At high temperatures (Fig. 4a), $v(F, T)$ varies smoothly with $F$ and no transition is observed, similar to the 0D case of a single pendulum. However, at low temperatures (Fig. 4b), $v(F, T)$ displays hysteretic behaviour as one sweeps the force. By increasing the timescale of each sweep (for example, increasing the number of driving periods at each $F$ from $n_{steps}=5\times10^3$ to $3\times10^6$), the hysteresis loop closes into a single-valued curve that exhibits an apparent jump discontinuity. This suggests that the interactions have transformed the bistable region II of the individual pendula into a finite-temperature first-order dynamical phase transition of the coupled chain. As an additional test, one can fix $F$ to its value near the transition and slowly vary $T$, reproducing the same discontinuous jump (Fig. 4d).

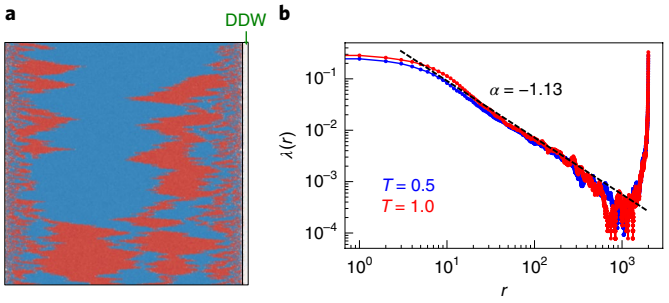


**Fig. 6 | The presence of power-law correlations at the first-order CDTC transition. a**, To probe these correlations, we pin a pair of dynamical domain walls by spatially modulating $F$ above and below $F_c$ (note the small white strip on the right, which is the high-$F$ region), and observe the resulting dynamics $q_j(2nt_D)$. The DDW emits a constant stream of π-domain walls into the CDTC region, visible as boundaries between red and blue domains. Their density is quantified by the average velocity $v(r) = \langle \dot{\tilde{\theta}}(r) \rangle$. **b**, The density of π-domain walls follows a power law $v(r) \approx r^{-\alpha}$ away from the DDW, where $\alpha \approx 1.13$. The exponent appears to be constant over several temperatures (here $T = 0.5$ and 1).

Although the jump looks sharp to the eye, it is difficult to numerically locate the transition in this manner, because the time required to close the hysteresis loop diverges at low temperature. To ameliorate this issue, we study the behaviour of a 'dynamical' domain wall (DDW) between the period-doubled and undoubled states, because presumably it is the nucleation of the first such DDW that requires the largest time. Specifically, we initialize the left half of the system to be in the symmetry-unbroken state with $q, p \approx 0$ and the right half of the system to be in the period-doubled CDTC with $q, p \approx \sqrt{2\bar{J}}$ (Fig. 5a). We then time evolve for $n_{steps} = 10^6$ to determine which state 'wins'. In Fig. 5b,c, we fix $T = 3.7$ and repeat this experiment for a very narrow window of $F$ around the putative transition at $F_c$. For $F < F_c$, we observe the CDTC region expand and 'eat' the non-time-crystalline region, while for $F > F_c$ we see the opposite behaviour. Meanwhile, close to the critical point, $F_c$, the competition between the two phases extends for many steps as the location of the DDW fluctuates, indicating coexistence[76].

To quantify this competition between the two domains, we measure the average oscillator amplitude, $\langle J(t) \rangle$, as the system evolves after the quench (Fig. 5c). Because $J$ differs between the CDTC and symmetry-unbroken states, its spatial average indicates which domain is winning (although other local observables would serve just as well). Far from $F_c$, $J$ converges rapidly in time to the value it takes in either the CDTC ($F < F_c$) or symmetry-unbroken ($F > F_c$) state, indicating that one or the other domain has taken over. As $F \to F_c$, the time required for convergence increases, and we utilize the long-time behaviour to accurately determine $F_c$. One expects that for larger systems, this convergence timescale will diverge, owing to the diffusive dynamics of the DDW, although we have not investigated this quantitatively[76].

By repeating this analysis as a function of $F$ and $T$, we obtain the CDTC phase diagram depicted in Fig. 2b. We observe a line of first-order dynamical phase transitions terminating at a point in the ($F$, $T$)-plane. As expected, in the CDTC region of the phase diagram, the rate of phase slips exhibits activated behaviour, $v \approx e^{-\Delta_{eff}(F)/T}$ (Fig. 2c), while at the first-order transition, $v$ jumps discontinuously into a regime with complete destruction of period-doubling.

The nature of the end-point of the first-order line is an intriguing question for future study. In Fig. 2d, we show the magnitude of the jump discontinuity, $\Delta v$, across the first-order line for a range of temperatures. The magnitude of the jump decreases as we approach the end-point of the first-order line, consistent with a scenario in which the phase transition becomes continuous at the critical end-point. Understanding this critical point would be a fruitful starting point for a field-theoretic understanding of the CDTC transition.

If the coarse-grained behaviour of the DDWs were governed by an effective free-energy functional with short-range interactions, then entropic arguments would imply that the putative transition is in fact rounded out to a crossover[57]. However, far from equilibrium, it is unclear that such a free-energy-based argument has any relevance. Moreover, a non-equilibrium system can generically develop power-law correlations, which may mediate power-law interactions between the DDWs. To explore this, we pin a pair of DDWs by spatially modulating $F$ slightly above and below its critical value. As depicted in Fig. 6a, we find that the DDW boundary between the CDTC and symmetry-unbroken regions emits a finite density of π-phase slips. These π-phase slips contribute to a finite velocity, $v(r)$, that depends on the distance $r$ from the DDW. We observe $v(r) \approx r^{-\alpha}$ over almost two decades, where $\alpha \approx 1.13$ (Fig. 6b); within the accuracy of our numerics, we obtain the same exponent $\alpha$ for cuts across the transition at two different temperatures $T = 0.5$ and 1. This power-law behaviour is certainly distinct from the expectations for an equilibrium first-order transition.

Finally, we will now consider a diagnostic of the CDTC phase that is particularly amenable to experiments (see Supplementary Information), namely the power spectrum of $q_j$; in the Supplementary Information, we propose two possible experimental realizations of our model using either a trapped-ion nanofriction simulator or a coupled array of superconducting junctions[77–79]. We define the 'stroboscopic' Fourier transform by $q(\omega, k) \equiv \sum_{n,j} (-1)^n e^{i(\omega n - kj)} q_j(nt_D)$. To estimate the power spectrum, $S(\omega, k) = \langle q(-\omega, -k) q(\omega, k) \rangle / n_{osc} n_{steps}$, we utilize Welch's method and average over the stochastic noise[80]. A typical spectral function is illustrated in Fig. 7a and reveals the dispersion relation of the effective Hamiltonian in equation (13).

Perfect ferromagnetic period-doubling would manifest as a $\delta$-function peak at $\omega$, $k = 0$. A shift in the peak (away from $\omega = 0$) indicates unlocking from the subharmonic response $\omega_D/2$. Because $(-1)^n q(nt_D) \approx \sqrt{2\bar{J}} \cos(\tilde{\theta}(t))$, this shift is precisely the velocity $v = \langle \dot{\tilde{\theta}} \rangle$ we have discussed, while the broadening is analogous to a Debye–Waller factor. In Fig. 7b, we depict $S(\omega, 0)$ for a range of temperatures across the phase transition and observe a qualitative transformation below $T_c$. As the temperature decreases even further, the spectral function has to be averaged over extremely long times in order to detect the exponentially small shift and broadening of the peak away from $\omega = 0$; nevertheless, it can be used to experimentally detect the first-order jump in $v$ shown in Fig. 4d.

## Discussion

We have demonstrated that a periodically driven, 1D system at finite temperature can exhibit a first-order dynamical phase transition between an activated classical discrete time crystal and a symmetry-unbroken phase. This behaviour depends crucially on an interplay between interactions and non-equilibrium driving, without which a transition would be forbidden.

Our work opens the door to a number of intriguing future directions. First, while the 1D CDTC model studied here is thermally activated, our understanding of Gács' result suggests that true CDTCs are, in principle, possible. If so, is there a simple 'physical' model, like the driven FK chain studied here, that exhibits a true CDTC, or is the whole complexity of the Gács result required?

In $d > 1$, where ergodicity can certainly be broken without requiring the full complexity of Gács' result (for example, in Toom's model[53]), the possibility of a true CDTC is still complex. This issue was considered in the context of certain 2D PCAs, where it has been argued that a higher-order subharmonic response (for example periodic tripling, $k = 3$) cannot have an

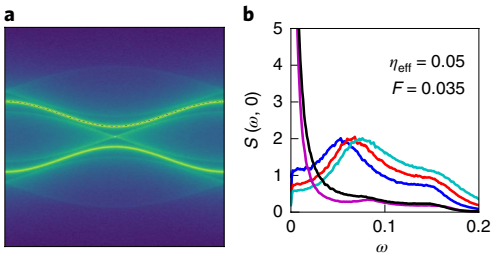


**Fig. 7 | Probing the CDTC using the stroboscopic spectral function.** **a**, The stroboscopic spectral function $S(\omega, k) \propto \langle |\mathrm{DFT}(-1)^n q_j(nt_D)|^2 \rangle$. In this convention, the period-doubled component is mapped to $\omega = k = 0$. Because the autocorrelation time is unmeasurable over the $n_{steps} = 15{,}000$ used to take the data, there is a $\delta$-function peak at the origin we have removed by hand to preserve the scale. The residual noise spectrum reveals the mode $\omega_{eff}(k)$ of the effective Floquet–Magnus Hamiltonian equation (13). **b**, $S(\omega, 0)$ as a function of frequency at several temperatures, holding the other parameters (for example, $F$, $\eta$, $g$) fixed. The lowest temperatures (purple, black) lie below the first-order transition, $T < T_c$, and the peaks (if resolved) would exhibit a very small shift away from $\omega = 0$ due to the exponentially rare activated phase slips. For the remaining curves $T > T_c$, and the peaks are strongly shifted away from $\omega = 0$, indicating unlocking of the subharmonic response.

infinite autocorrelation time, while a period-doubled response could[56]. The basic argument is that if a fluctuation nucleates a bubble of the neighbouring subharmonic orbit (the generalization of our π-phase slips), the domain wall will generically experience a force that causes the bubble to expand, destroying the CDTC. They argue that this force is absent for $k = 2$ because an Ising-like domain wall does not have an orientation, leading to the distinction between $k = 2$ and $k > 2$.

Our mapping to a tilted sine-Gordon model provides a new perspective on their analysis. For a $k$th-order subharmonic response, as would occur for a $k$:1 parametric resonance, one can generalize our effective Hamiltonian by simply replacing the period of the washboard potential with $\cos(k\tilde{\theta}_j)$. As we have emphasized, when the domain wall is smooth, it still has a definite handedness even when $k = 2$, so the distinction between $k = 2$ and $k > 2$ no longer seems so important. Indeed, in the continuum limit, $k$ drops out of the resulting sine-Gordon model. For a tilted sine-Gordon model satisfying detailed balance, the 'locked' phase, with true long-range order at the subharmonic period, is unstable in any dimension: that is, for any non-zero tilt there is only a finite energy barrier to create a phase slip domain, which, once nucleated, grows rapidly to infinite size due to the tilt. However, nucleation could, in principle, be prevented by non-equilibrium effects. Furthermore, the locking to a commensurate frequency and the existence of spontaneous oscillations are potentially distinct: even the 'sliding' phase may exhibit long-range or quasi-long-range[81] order at a frequency shifted from $\omega_D/2$. Such 'incommensurate' temporal order has been discussed in the context of driven periodic media[20].

Furthermore, while the handedness (and hence force) on domain walls is well defined in the sine-Gordon continuum limit, the lattice allows for 2π-vortices at which the orientation of the domain wall reverses. These vortices cost finite energy when localized to the domain wall, where they may proliferate due to fluctuations. This may provide a mechanism that renormalizes the force on the domain walls to zero, stabilizing a true CDTC for $k = 2$ and $d > 1$.

Another interesting scenario is to consider the $\eta$, $T \to 0$ limit of our model, which reduces to closed Hamiltonian dynamics. Here, we observe that the dynamics remain period-doubled out to extremely long timescales (for example, many millions of driving cycles). This behaviour appears to be the classical analogue[82,83] of a 'prethermal' time crystal and arises from a mismatch between the driving frequency $\omega_D$ and the effective resonance frequency $\omega_{eff}$ (refs. [33,65,82–84]).

The existence of a first-order line terminating at a critical point is reminiscent of the equilibrium liquid–gas transition. To this end, at the critical point, one might hope to develop a non-equilibrium field theory for the transition within the Martin–Siggia–Rose path integral formalism[85,86]. Such a field theory might also be used to determine the precise relation between classical and quantum time crystals by analysing the semiclassical limit of its Keldysh path integral.

Finally, we comment on the relation of CDTC order to synchronization transitions, which arise, for example, in the Kuramoto model[12]. Adding a weak external periodic drive to a synchronized model, at a frequency that is a multiple of the synchronized one, presumably converts the synchronized phase into a rigid subharmonic response[1]. However, this does not mean the Kuramoto model is an example of a CDTC. First, the Kuramoto model is usually understood as an all-to-all model, which is non-local, so one needs to begin by introducing a geometry to the couplings (chain, array, and so on). Second, the usual Kuramoto model is dissipative, for which we have emphasized there are already many examples of rigid subharmonic responses. So one should either (1) consider the Hamiltonian realization of the Kuramoto model, with no friction[87] (the closed case) or (2) couple the model to spatio-temporal noise[88], for example a Langevin force (the open case). The stability of synchronization, in the sense of an infinite autocorrelation time, in a local model is to our knowledge unknown for both the closed and open cases[88].

## Online content

Any methods, additional references, Nature Research reporting summaries, source data, extended data, supplementary information, acknowledgements, peer review information; details of author contributions and competing interests; and statements of data and code availability are available at https://doi.org/10.1038/s41567-019-0782-3.

Received: 16 June 2018; Accepted: 16 December 2019;
Published online: 10 February 2020

## References

1. Van der Pol, B. & Van Der Mark, J. Frequency demultiplication. *Nature* **120**, 363–364 (1927).
2. May, R. M. Simple mathematical models with very complicated dynamics. *Nature* **261**, 459–467 (1976).
3. Cross, M. C. & Hohenberg, P. C. Pattern formation outside of equilibrium. *Rev. Mod. Phys.* **65**, 851–1112 (1993).
4. Brown, S. E., Mozurkewich, G. & Grüner, G. Subharmonic Shapiro steps and devil's-staircase behavior in driven charge-density-wave systems. *Phys. Rev. Lett.* **52**, 2277–2280 (1984).
5. Parlitz, U., Junge, L. & Kocarev, L. Subharmonic entrainment of unstable period orbits and generalized synchronization. *Phys. Rev. Lett.* **79**, 3158–3161 (1997).
6. Rasband, S. N. *Chaotic Dynamics of Nonlinear Systems* (Dover Publications, 2015).
7. Strogatz, S. H. *Nonlinear Dynamics and Chaos: With Applications to Physics, Biology, Chemistry, and Engineering* (Westview Press, 2014).
8. Linsay, P. S. Period doubling and chaotic behavior in a driven anharmonic oscillator. *Phys. Rev. Lett.* **47**, 1349–1352 (1981).
9. Kaneko, K. Period-doubling of kink–antikink patterns, quasiperiodicity in antiferro-like structures and spatial intermittency in coupled logistic lattice: towards a prelude of a 'field theory of chaos'. *Prog. Theor. Phys.* **72**, 480–486 (1984).
10. Jackson, E. A. & Hübler, A. Periodic entrainment of chaotic logistic map dynamics. *Physica D* **44**, 407–420 (1990).
11. Van der Pol, B. LXXXVIII. On "relaxation-oscillations". *Lond. Edinb. Dubl. Phil. Mag.* **2**, 978–992 (1926).
12. Kuramoto, Y. Self-entrainment of a population of coupled non-linear oscillators. In *Int. Symposium on Mathematical Problems in Theoretical Physics* 420–422 (Springer, 1975).

13. Gupta, S., Campa, A. & Ruffo, S. Nonequilibrium first-order phase transition in coupled oscillator systems with inertia and noise. *Phys. Rev. E* **89**, 022123 (2014).
14. Brown, S. E., Mozurkewich, G. & Grüner, G. Harmonic and subharmonic Shapiro steps in orthorhombic $TaS_3$. *Solid State Commun.* **54**, 23–26 (1985).
15. Tua, P. & Ruvalds, J. Dynamics of driven charge-density waves: subharmonic Shapiro steps with devil's staircase structure. *Solid State Commun.* **54**, 471–474 (1985).
16. Sherwin, M. & Zettl, A. Complete charge density-wave mode locking and freeze-out of fluctuations in $NbSe_3$. *Phys. Rev. B* **32**, 5536–5539 (1985).
17. Wiesenfeld, K. & Satija, I. Noise tolerance of frequency-locked dynamics. *Phys. Rev. B* **36**, 2483–2492 (1987).
18. Bhattacharya, S., Stokes, J. P., Higgins, M. J. & Klemm, R. A. Temporal coherence in the sliding charge-density-wave condensate. *Phys. Rev. Lett.* **59**, 1849–1852 (1987).
19. Falo, F., Floría, L. M., Martínez, P. J. & Mazo, J. J. Unlocking mechanism in the ac dynamics of the Frenkel–Kontorova model. *Phys. Rev. B* **48**, 7434–7437 (1993).
20. Balents, L. & Fisher, M. P. Temporal order in dirty driven periodic media. *Phys. Rev. Lett.* **75**, 4270–4273 (1995).
21. Tekić, J., He, D. & Hu, B. Noise effects in the ac-driven Frenkel-Kontorova model. *Phys. Rev. E* **79**, 036604 (2009).
22. Tekić, J. et al. *The ac driven Frenkel-Kontorova Model* (Vinča Nuclear Institute, 2016).
23. Lee, H. C. et al. Subharmonic Shapiro steps in Josephson-junction arrays. *Phys. Rev. B* **44**, 921–924 (1991).
24. Yu, W., Harris, E. B., Hebboul, S. E., Garland, J. C. & Stroud, D. Fractional Shapiro steps in ladder Josephson arrays. *Phys. Rev. B* **45**, 12624–12627 (1992).
25. Wilczek, F. Quantum time crystals. *Phys. Rev. Lett.* **109**, 160401 (2012).
26. Shapere, A. & Wilczek, F. Classical time crystals. *Phys. Rev. Lett.* **109**, 160402 (2012).
27. Bruno, P. Impossibility of spontaneously rotating time crystals: a no-go theorem. *Phys. Rev. Lett.* **111**, 070402 (2013).
28. Nozières, P. Time crystals: can diamagnetic currents drive a charge density wave into rotation? *Europhys. Lett.* **103**, 57008 (2013).
29. Volovik, G. E. On the broken time translation symmetry in macroscopic systems: precessing states and off-diagonal long-range order. *JETP Lett.* **98**, 491–495 (2013).
30. Sacha, K. Modeling spontaneous breaking of time-translation symmetry. *Phys. Rev. A* **91**, 033617 (2015).
31. Watanabe, H. & Oshikawa, M. Absence of quantum time crystals. *Phys. Rev. Lett.* **114**, 251603 (2015).
32. Heo, M.-S. et al. Ideal mean-field transition in a modulated cold atom system. *Phys. Rev. E* **82**, 031134 (2010).
33. Citro, R. et al. Dynamical stability of a many-body Kapitza pendulum. *Ann. Phys.* **360**, 694–710 (2015).
34. Chandran, A. & Sondhi, S. L. Interaction-stabilized steady states in the driven $O(N)$ model. *Phys. Rev. B* **93**, 174305 (2016).
35. Liggett, T. M. *Interacting Particle Systems* Vol. 276 (Springer, 2012).
36. Khemani, V., Lazarides, A., Moessner, R. & Sondhi, S. L. Phase structure of driven quantum systems. *Phys. Rev. Lett.* **116**, 250401 (2016).
37. Else, D. V., Bauer, B. & Nayak, C. Floquet time crystals. *Phys. Rev. Lett.* **117**, 090402 (2016).
38. von Keyserlingk, C. W., Khemani, V. & Sondhi, S. L. Absolute stability and spatiotemporal long-range order in Floquet systems. *Phys. Rev. B* **94**, 085112 (2016).
39. Yao, N. Y., Potter, A. C., Potirniche, I.-D. & Vishwanath, A. Discrete time crystals: rigidity, criticality and realizations. *Phys. Rev. Lett.* **118**, 030401 (2017).
40. Khemani, V., vonKeyserlingk, C. W. & Sondhi, S. L. Defining time crystals via representation theory. *Phys. Rev. B* **96**, 115127 (2017).
41. Lazarides, A. & Moessner, R. Fate of a discrete time crystal in an open system. *Phys. Rev. B* **95**, 195135 (2017).
42. Iemini, F. et al. Boundary time crystals. *Phys. Rev. Lett.* **121**, 035301 (2018).
43. Else, D. V., Monroe, C., Nayak, C. & Yao, N. Y. Discrete time crystals. Preprint at https://arxiv.org/pdf/1905.13232.pdf (2019).
44. Yao, N. Y. & Nayak, C. Time crystals in periodically driven systems. *Phys. Today* **71**, 40–47 (2018).
45. Zhang, J. et al. Observation of a discrete time crystal. *Nature* **543**, 217–220 (2017).
46. Choi, S. et al. Observation of discrete time-crystalline order in a disordered dipolar many-body system. *Nature* **543**, 221–225 (2017).
47. Rovny, J., Blum, R. L. & Barrett, S. E. Observation of discrete-time-crystal signatures in an ordered dipolar many-body system. *Phys. Rev. Lett.* **120**, 180603 (2018).
48. Rovny, J., Blum, R. L. & Barrett, S. E. $^{31}$P NMR study of discrete time-crystalline signatures in an ordered crystal of ammonium dihydrogen phosphate. *Phys. Rev. B* **97**, 184301 (2018).
49. Nyquist, H. Thermal agitation of electric charge in conductors. *Phys. Rev.* **32**, 110–113 (1928).
50. Gács, P. Reliable computation with cellular automata. *J. Comput. Syst. Sci.* **32**, 15–78 (1986).
51. Gács, P. Reliable cellular automata with self-organization. *J. Stat. Phys.* **103**, 45–267 (2001).
52. Gray, L. F. A reader's guide to Gacs's 'positive rates' paper. *J. Stat. Phys.* **103**, 1–44 (2001).
53. Toom, A. L. Nonergodic multidimensional system of automata. *Problemy Peredachi Informatsii* **10**, 70–79 (1974).
54. Toom, A. Unstable multicomponent systems. *Problemy Peredachi Informatsii* **12**, 78–84 (1976).
55. Toom, A. Stable and attractive trajectories in multicomponent systems. *Adv. Probab.* **6**, 549–575 (1980).
56. Bennett, C. H., Grinstein, G., He, Y., Jayaprakash, C. & Mukamel, D. Stability of temporally periodic states of classical many-body systems. *Phys. Rev. A* **41**, 1932–1935 (1990).
57. Landau, L. D. & Lifshitz, E. M. *Statistical Physics Vol. 5: Course of Theoretical Physics* (Pergamon Press, 1969).
58. Wolfram, S. Statistical mechanics of cellular automata. *Rev. Mod. Phys.* **55**, 601–644 (1983).
59. Frenkel, J. & Kontorova, T. On the theory of plastic deformation and twinning. *Izv. Akad. Nauk Fiz.* **1**, 137–149 (1939).
60. Braun, O. M. & Kivshar, Y. S. *The Frenkel–Kontorova Model: Concepts, Methods, and Applications* (Springer Science & Business Media, 2013).
61. Zounes, R. S. & Rand, R. H. Subharmonic resonance in the non-linear Mathieu equation. *Int. J. Non-Linear Mech.* **37**, 43–73 (2002).
62. Brizard, A. J. Jacobi zeta function and action-angle coordinates for the pendulum. *Commun. Nonlinear Sci. Numer. Simul.* **18**, 511–518 (2013).
63. Stewart, W. Current–voltage characteristics of Josephson junctions. *Appl. Phys. Lett.* **12**, 277–280 (1968).
64. McCumber, D. E. Effect of ac impedance on dc voltage–current characteristics of superconductor weak-link junctions. *J. Appl. Phys.* **39**, 3113–3118 (1968).
65. Else, D. V., Bauer, B. & Nayak, C. Prethermal phases of matter protected by time-translation symmetry. *Phys. Rev. X* **7**, 011026 (2017).
66. Hänggi, P., Talkner, P. & Borkovec, M. Reaction-rate theory: fifty years after Kramers. *Rev. Mod. Phys.* **62**, 251–341 (1990).
67. Büttiker, M., Harris, E. P. & Landauer, R. Thermal activation in extremely underdamped Josephson-junction circuits. *Phys. Rev. B* **28**, 1268–1275 (1983).
68. Dykman, M. I., Maloney, C. M., Smelyanskiy, V. N. & Silverstein, M. Fluctuational phase-flip transitions in parametrically driven oscillators. *Phys. Rev. E* **57**, 5202–5212 (1998).
69. Purcell, E. M. & Pound, R. V. A nuclear spin system at negative temperature. *Phys. Rev.* **81**, 279 (1951).
70. Braun, S. et al. Negative absolute temperature for motional degrees of freedom. *Science* **339**, 52–55 (2013).
71. Nakagawa, M., Tsuji, N., Kawakami, N. & Ueda, M. Negative-temperature quantum magnetism in open dissipative systems. Preprint at https://arxiv.org/abs/1904.00154 (2019).
72. Kapitza, P. L. A pendulum with oscillating suspension. *Uspekhi Fizicheskikh Nauk* **44**, 7–20 (1951).
73. Braun, O. M., Dauxois, T., Paliy, M. V. & Peyrard, M. Nonlinear mobility of the generalized Frenkel–Kontorova model. *Phys. Rev. E* **55**, 3598–3612 (1997).
74. Braun, O., Bishop, A. & Röder, J. Hysteresis in the underdamped driven Frenkel–Kontorova model. *Phys. Rev. Lett.* **79**, 3692–3695 (1997).
75. Zheng, Z., Hu, B. & Hu, G. Resonant steps and spatiotemporal dynamics in the damped dc-driven Frenkel-Kontorova chain. *Phys. Rev. B* **58**, 5453–5461 (1998).
76. Huse, D. A. & Fisher, D. S. Dynamics of droplet fluctuations in pure and random Ising systems. *Phys. Rev. B* **35**, 6841–6846 (1987).
77. Vanossi, A., Manini, N., Urbakh, M., Zapperi, S. & Tosatti, E. Colloquium: modeling friction: from nanoscale to mesoscale. *Rev. Mod. Phys.* **85**, 529–552 (2013).
78. Bylinskii, A., Gangloff, D. & Vuletić, V. Tuning friction atom-by-atom in an ion-crystal simulator. *Science* **348**, 1115–1118 (2015).
79. Masluk, N. A., Pop, I. M., Kamal, A., Minev, Z. K. & Devoret, M. H. Microwave characterization of Josephson junction arrays: implementing a low loss superinductance. *Phys. Rev. Lett.* **109**, 137002 (2012).
80. Welch, P. The use of fast Fourier transform for the estimation of power spectra: a method based on time averaging over short, modified periodograms. *IEEE Trans. Audio Electroacoust.* **15**, 70–73 (1967).
81. Grinstein, G., Mukamel, D., Seidin, R. & Bennett, C. H. Temporally periodic phases and kinetic roughening. *Phys. Rev. Lett.* **70**, 3607–3610 (1993).
82. Rajak, A., Citro, R. & DallaTorre, E. G. Stability and pre-thermalization in chains of classical kicked rotors. *J. Phys. A* **51**, 465001 (2018).

83. Mori, T. Floquet prethermalization in periodically driven classical spin systems. *Phys. Rev. B* **98**, 104303 (2018).
84. Abanin, D. A., De Roeck, W., Ho, W. W. & Huveneers, Fmc Effective Hamiltonians, prethermalization and slow energy absorption in periodically driven many-body systems. *Phys. Rev. B* **95**, 014112 (2017).
85. Martin, P. C., Siggia, E. D. & Rose, H. A. Statistical dynamics of classical systems. *Phys. Rev. A* **8**, 423–437 (1973).
86. Sieberer, L. M. & Altman, E. Topological defects in anisotropic driven open systems. *Phys. Rev. Lett.* **121**, 085704 (2018).
87. Witthaut, D. & Timme, M. Kuramoto dynamics in Hamiltonian systems. *Phys. Rev. E* **90**, 032917 (2014).
88. Acebrón, J. A., Bonilla, L. L., Vicente, C. J. P., Ritort, F. & Spigler, R. The Kuramoto model: a simple paradigm for synchronization phenomena. *Rev. Mod. Phys.* **77**, 137–186 (2005).

## Data availability

The data represented in Figs. 2b–d, 4a–d, 6b and 7b are available as Source Data. All other data that support the plots within this paper and other findings of this study are available from the corresponding author upon reasonable request.

## Acknowledgements

We gratefully acknowledge the insights of and discussions with E. Altman, D. Huse, S. Gazit, R. Goldstein, L. Sieberer, S. Sondhi and B. Zhu. This work was supported, in part, by the DARPA DRINQS programme (D18AC00033), the David and Lucile Packard Foundation and the W. M. Keck Foundation. L.B. was supported by the NSF Materials Theory programme through grant DMR1506119.

## Author contributions

All authors contributed extensively to all aspects of this work.

## Competing interests

The authors declare no competing interests.

## Additional information

**Supplementary information** is available for this paper at https://doi.org/10.1038/s41567-019-0782-3.

**Correspondence and requests for materials** should be addressed to N.Y.Y.

**Peer review information** *Nature Physics* thanks Dmitry Abanin, Emanuele Dalla Torre and the other, anonymous, reviewer(s) for their contribution to the peer review of this work.

**Reprints and permissions information** is available at www.nature.com/reprints.